OPTIMAL ALLOCATION OF TCSC DEVICES FOR THE ENHANCEMENT OF ATC IN DEREGULATED POWER SYSTEM USING FLOWER POLLINATION ALGORITHM

K. T. VENKATRAMAN[1,*], B. PARAMASIVAM[2], I. A. CHIDAMBARAM[3]

[1]Department of EEE, Government Polytechnic College,
Korukkai, Tamilnadu, India
[2]Department of EEE, Government College of Engineering,
Bodinayakkanur, Tamilnadu, India
[3]Department of Electrical Engineering, Annamalai University, Annamalainagar,
Tamilnadu, India
*Corresponding Author: ktvaeee@gmail.com

Abstract

This paper proposes a best possible distribution of Thyristor Controlled Series Compensator (TCSC) to progress the Available Transfer Capability (ATC) of power transactions between sources and sink areas in the deregulated power system. The principle of TCSC device is to balance the inductive voltage drop in the line by an introduced capacitive voltage or in other words to alleviate the effective reactance of the transmission line to improve ATC in the network. The objective of the optimization is to find the preeminent location and parameters of TCSC devices by means of Flower Pollination Algorithm (FPA) for maximizing ATC and minimizing power losses and installation cost of TCSC device. The estimate of ATC using AC Power Transfer Distribution Factors (ACPTDF) based on the Newton Raphson power flow technique. The ACPTDFs are the consequent using sensitivity based approach for the system intact case and utilized to check the line flow limits during ATC fortitude. The efficacy of the proposed method is demonstrated using an IEEE-30 bus test system for the evaluation of ATC in normal and line outage contingencies conditions for the preferred bilateral, multilateral and area wise transactions. The simulation outcome illustrates that the introduction of TCSC devices in an accurate location could increase ATC, fall in total losses and advance the line congestion as compared to the system without TCSC devices.

Keywords: ACPTDF, ATC, FPA, TCSC.

1. Introduction

The focus of deregulation is to provide an element of a race with electrical energy delivery and allow the market price of energy at low rates to the customer with higher efficiency from the suppliers. In a deregulated environment, all parties may try to generate the energy from the cheaper source for higher profit edge, which may lead to overloading and congestion of positive corridors of the transmission network. This may effect in violation of line flow, voltage and stability limits and thereby weaken the system security. Utilities need to establish adequately their ATC to ensure the system reliability is maintained while serving a wide range of bilateral and multilateral transactions [1, 2]. Many methods have been recommended to evaluate the ATC and these methods are different on the basis of the power flow model, the system aspects considered, the persuasive limits under consideration and few other aspects. However, a wide way of categorizing the methods is based on the type of limit considered, i.e., thermal limit, voltage limit or the angular stability limit. ATC is estimated based on Continuation Power Flow (CPF) and Repeated Power Flow (RPF), which provide very precise ATC, results as it considers system non-linearity and control changes. The limitations of the above-said methods are not suitable for large power system and it cannot be applied to real-time applications due to computational complexity [3].

Many authors provide the estimate of ATC based on the power flow sensitivity method [4-8]. Linear sensitivity factors are engaged for the rapid calculation of ATC and these factors give the approximate change in line flows for changes in the generation of the system. Linear sensitivity factors use DC Power Transfer Distribution Factors (DCPTDFs) and Line Outage Power Transfer Distribution Factors (LOPTDFs) obtained from the DC load flow [4]. DCPTDFs are easy to calculate ATC and offers quick computations. But it provides less accurate DC power flow voltage, reactive power effects and more accurate PTDFs can be calculated using the AC power flow model. Line power flows are basically a function of the voltages and angles at its terminal buses. So PTDF is a function of these voltage and angle sensitivities. AC Power Transfer Distribution Factors (ACPTDFs) are also projected for ATC determination [5, 6]. ACPTDFs are derived from the base operating point using AC load flow analysis with consideration of reactive power limits and voltage limits and it gives more accurate ATC with lower computation complexity. In this study, the estimation of ATC by means of ACPTDFs based approach has been suggested for single and simultaneous transactions calculated using the *N-R* method.

The performance of the power flows in the network is increased by Flexible Alternative Current Transmission System (FACTS) devices without generation rescheduling or topological changes. The use of FACTS devices in electrical systems appears to be a hopeful scheme to decline the transmission congestion and raise the ATC [8-10]. A series connected TCSC is able of incessantly changing the impedance to control the power flow can augment ATC and perk up the line congestion. The main idea of this study includes the optimal location of the TCSC devices placement for enhancement of ATC thereby reduction of losses and TCSC device investment cost. Various researchers are used Artificial Intelligence (AI) based Genetic Algorithm (GA), Particle Swarm Optimization (PSO) and Harmony Search Algorithm (HSA) techniques in order to improve the ATC with the optimal locations, installation cost and parameters setting of FACTS devices between generators and loads without violating system constraints [11-15]. A newly

developed Flower Pollination Algorithm (FPA) is a metaheuristic optimization technique founded on pollination of flowers has only one key parameter *p* (switch probability), which makes the algorithm easy to apply and enable to reach quick optimum solution [16]. FPA technique has exclusive capability such as wide province search with distinction and reliable solution [17]. In this study, FPA is used to discover the best location and control parameters of TCSC devices to attain the highest value of ATC with reduced line congestion and total power loss.

2. ATC Evaluation using AC Power Transfer Distribution Factors

ATC is a measure of the residual transfer capability in the physical transmission network for additional commercial activity over and above previously committed uses [4]. Mathematically, ATC is defined as:

$$ATC = TTC - ETC - CBM - TRM \tag{1}$$

The estimate of ATC using PTDF is simple and less time-consuming. There are different sensitivity factors existing in the literature to analyse ATC for a certain system [8]. Basically, these factors provide the correlation between the quantity of transaction and the actual power flow in a line. In this study, AC load flow study based PTDF is used to recognize the system parameter for a change in MW transaction under normal and contingency conditions. Let us considered a bilateral transaction t_k, the change in real power transactions between the seller '*m*' and buyer '*n*', say by Δt_k MW and due to this, the change in real power flow in a transmission line connected between buses *i* and *j* is ΔP. From this, ACPTDF can be defined as:

$$ACPTDF_{ij,mn} = \frac{\Delta P}{\Delta t_k} \tag{2}$$

ACPTDF are evaluate using base case load flow results using Newton-Raphson-Jacobian elements $[J_T]$ and expressed as

$$\begin{bmatrix} \Delta \delta \\ \Delta V \end{bmatrix} = \begin{bmatrix} \frac{\partial P}{\partial \delta} & \frac{\partial P}{\partial V} \\ \frac{\partial Q}{\partial \delta} & \frac{\partial Q}{\partial V} \end{bmatrix}^{-1} \begin{bmatrix} \Delta P \\ \Delta Q \end{bmatrix} = [J_T]^{-1} \begin{bmatrix} \Delta P \\ \Delta Q \end{bmatrix} \tag{3}$$

The power change in a transaction causes the change of active power flow in line *i–j*. These changes can be mathematically represented as:

$$\frac{\partial P_{ij}}{\partial \delta_m} = \begin{cases} -V_i V_j Y_{ij} \sin(\delta_i - \delta_j - \theta_{ij}) form = i \\ V_i V_j Y_{ij} \sin(\delta_i - \delta_j - \theta_{ij}) form = j \\ 0 \, form \neq i, j \end{cases} \tag{4}$$

$$\frac{\partial P_{ij}}{\partial V_m} = \begin{cases} 2V_i V_j Y_{ij} \cos(\theta_{ij}) + V_j Y_{ij} cos(\delta_i - \delta_j - \theta_{ij}) form = i \\ V_j Y_{ij} \cos(\delta_i - \delta_j - \theta_{ij}) form = j \\ 0 \, form \neq i, j \end{cases} \tag{5}$$

In the bi-lateral transaction, due to change in Δt_k MW, the following two mismatch vectors are changed in Eq. (3) and these values are non-zero elements.

$$\Delta P_i = \Delta t_k \quad ; \; \Delta P_j = -\Delta t_k \tag{6}$$

Based on these mismatch vectors and change in power transactions are considered to calculate the new voltage magnitudes and angles at all buses. The change in power flows in all the Transmission Lines (N_L) is calculated using new voltage profiles. The

ACPTDF in each line for a given transaction is evaluating using Eq. (2) and ATC of a transaction between buses '*m*' and '*n*' can be calculated as given by:

$$ATC_{mn} = \min(T_{ij,mn}), ij \epsilon N_L \tag{7}$$

$T_{ij,mn}$ denotes the transfer limit values for each line in the system. It is given by

$$\begin{cases} \frac{(P_{ij}^{max} - P_{ij}^0)}{PTDF_{ij,mn}}; & PTDF_{ij,mn} > 0 \\ \frac{(-P_{ij}^{max} - P_{ij}^0)}{PTDF_{ij,mn}}; & PTDF_{ij,mn} < 0 \\ \infty; & PTDF_{i,mn} = 0 \end{cases} \tag{8}$$

where, P_{ij}^{max}, P_{ij}^0 are maximum power flow limit in MW and base case power flow of a line between bus i and j.

3. Static Modelling of TCSC Devices

The power flow equations of the line connected between bus i and bus j having a series impedance $r_{ij} + jx_{ij}$ and without any TCSC devices are given by:

$$P_{ij} = V_i^2 g_{ij} - V_i V_j (g_{ij} cos\delta_{ij} + b_{ij} sin\delta_{ij}) \tag{9}$$

$$Q_{ij} = -V_i^2 (b_{ij} + B_{sh}) - V_i V_j (g_{ij} sin\delta_{ij} - b_{ij} cos\delta_{ij}) \tag{10}$$

where V_i, V_j are the magnitudes voltage at bus-i and bus-j, δ_{ij} is the angle difference between bus-i and bus-j and $g_{ij} = \frac{r_{ij}}{r_{ij}^2 + x_{ij}^2}$, $b_{ij} = \frac{-x_{ij}}{r_{ij}^2 + x_{ij}^2}$. Similarly, the active power (P_{ji}) and reactive power (Q_{ji}) flow from bus-j and bus-i in the line given by:

$$P_{ji} = V_j^2 g_{ij} - V_i V_j (g_{ij} cos\delta_{ij} - b_{ij} sin\delta_{ij}) \tag{11}$$

$$Q_{ji} = -V_j^2 (b_{ij} + B_{sh}) + V_i V_j (g_{ij} sin\delta_{ij} + b_{ij} cos\delta_{ij}) \tag{12}$$

The power flow control with TCSC connected between bus-i and bus-j is shown in Fig. 1.
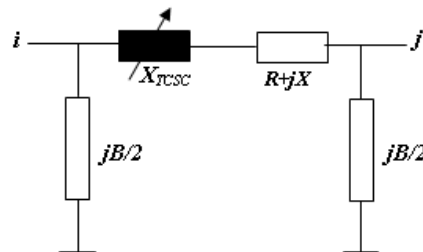
Fig. 1. Equivalent circuit of TCSC device.

The reactance of the line with TCSC is given by:

$$x_{ij} = x_{line} + x_{TCSC} \tag{13}$$

$$x_{TCSC} = \gamma_{TCSC} * x_{line} \tag{14}$$

where, X_{line} is the reactance of the transmission line and γ_{TCSC} is the compensation factor of TCSC. The real and reactive power flow from bus-i to bus-j and bus-j to bus-i in the line given by Eqs. (9) to (12) with modified g_{ij} and b_{ij} as given by:

$$g_{ij} = \frac{r_{ij}}{r_{ij}^2 + (x_{ij} - x_{TCSC})^2} \tag{15}$$

$$b_{ij} = \frac{-(x_{ij} - x_{TCSC})}{r_{ij}^2 + (x_{ij} - x_{TCSC})^2} \tag{16}$$

4. Problem Formulation

The objective is to maximize the ATC when a transaction is taking place between a seller bus (*m*) and buyer bus (*n*). The objective function to be maximized is given by:

$$J = Max \ (ATC_{mn})) \tag{17}$$

It is subjected to the following equality, in-equality and practical constraints.

$$P_{Gi} - P_{Di} - \sum_{j=1}^{nb} V_i V_j Y_{ij} \cos(\delta_i - \delta_j - \theta_{ij}) = 0 \tag{13}$$

$$Q_{Gi} - Q_{Di} - \sum_{j=1}^{nb} V_i V_j Y_{ij} \sin(\delta_i - \delta_j - \theta_{ij}) = 0 \tag{19}$$

where P_{Gi}, Q_{Gi} are the real and reactive power generations at i^{th} bus, P_{Di}, Q_{Di} are the real and reactive power demands at i^{th} bus, $Y_{ij}\theta_{ij}$ are the bus admittance magnitude and its angle between i^{th} and j^{th} buses, δ_i, δ_j are voltage angles of bus i and bus j respectively *nb*, n_g is the total number of buses and generator.

$$P_{Gi}^{min} \le P_{Gi} \le P_{Gi}^{max} \ for \ i = 1,2 \ldots \ldots n_g \tag{20}$$

$$Q_{Gi}^{min} \le Q_{Gi} \le Q_{Gi}^{max} \ for \ i = 1,2 \ldots \ldots n_g \tag{21}$$

$$V_b^{min} \le V_b \le V_b^{max} \ for \ i = 1,2 \ldots \ldots n_b \tag{22}$$

The practical constraints of the TCSC devices are [15]:

$$-0.8x_{line} \le x_{TCSC} \le 0.2x_{line} p.u. \tag{23}$$

where $_{TCSC}$ is the reactance added to the line by placing TCSC, x_{line} is the line reactance where TCSC is placed. To prevent overcompensation, TCSC reactance is chosen between $-0.8x_{line}$ to $0.2x_{line}$. The constraints on the installation cost of the corresponding TCSC devices are given in Eq. (24). The installation cost of TCSC is taken from [15].

$$C_{TCSC} = 0.0015S^2 - 0.713S + 153.75 US\$/KVAr \tag{24}$$

$$S = |Q_1| - |Q_2| \tag{25}$$

where Q_1 and Q_2 is the reactive power flow in the line without and with TCSC device in MVAr respectively.

5. Optimal Allocation of TCSC Devices using Flower Pollination Algorithm

5.1. Overview of flower pollination algorithm

Yang [16] suggested FPA based on flower pollination procedure of flowering plants. Flower pollination happens in two types namely self-pollination and cross-pollination. The self-pollination happens when pollen from one flower pollinates the similar flower or other flowers of the same plant. On the other hand, cross-pollination means pollination can occur from the pollen of a flower of a different plant. Biotic, cross-pollination occurring at a long distance may be called as the global pollination initiated by bees, bats, birds and flies, which could fly a long

distance. In the global pollination step, flower pollens are carried by pollinators such as insects, and pollens can travel over a long distance because insects can often fly and move in a much longer range. This ensures the pollination and reproduction of the fittest as g_* and represented mathematically as:

$$x_i^{t+1} = x_i^t + L(x_i^t - g_*) \tag{26}$$

where x_i^{t+1} is the solution vector x_i at iteration t, and g_* is the current best solution found among all solutions at the current generation/iteration. The parameter L is the strength of the pollination, which essentially is a step size [17] and mathematically denoted as:

$$L \sim \frac{\lambda \Gamma(\lambda) \sin\left(\frac{\pi\lambda}{2}\right)}{\pi} \frac{1}{s^{1+\lambda}} \qquad (s \gg s_0 > 0) \tag{27}$$

where $\Gamma(\lambda)$ is the standard gamma function and this distribution is valid for large steps $s > 0$. The local pollination and flower constancy can be denoted as:

$$x_i^{t+1} = x_i^t + \varepsilon\left(x_j^t - x_k^t\right) \tag{28}$$

where x_j^t and x_k^t are pollens from different flowers of the same plant species.

These basically mimic the flower constancy in a limited neighbourhood. Most flower pollination activities can occur at both local and global scale.

5.2. FPA based optimal allocation TCSC devices for ATC enhancement

The FPA for solving optimal allocation of TCSC devices is given as follows:

Step 1: Read the system input data.

Step 2: Initialize a population of n flowers. The initial population is generated from the following parameters; n_{FACTS}: the number of TCSC devices to be simulated; $n_{Location}$: the possible location for TCSC devices. In this study, the size of population $(n) = 15$

Step 3: Run a base case load flow.

Step 4: Initialize the objective function as given in Eq. (17).

Step 5: Consider wheeling transactions (t_k).

Step 6: Compute ACPTDF using Eq. (2).

Step 7: Take transactions as variables, line flow and real and reactive power limits of generators as constraints and compute the feasible wheeling transactions to determine the ATC as per Eq. (7).

Step 8: Find the limiting element in the system buses, i.e., that carry power close to the thermal limit.

Step 9: Place TCSC devices in the limiting element.

Step 10: Find the best solution g^* in the initial population

Step 11: Define a switching probability $p \in [0, 1]$ and define a stopping criterion (a fixed number of generations/iterations). The probability switch (p) =0.5 is considered in this study.

Step 12: while (t <Maximum Generation) for i= 1: n (all n flowers in the population) if rand <p, and draw a (d-dimensional) step vector L, which obeys a

levy distribution global pollination has been done using Eq. (26). Else, draw ε from a uniform distribution in [0, 1]. Randomly choose j^{th} and k^{th} flower among all the solutions and do local pollination through Eq. (28), end if.

Step 13: Evaluate new solutions using the objective function. If new solutions are better, update them in the population, end for.

Step 14: Find the current best solution g based on the objective fitness value, end while.

Step 15: Calculate ATC after incorporating TCSC devices.

Step 16: Is any other transaction has to be carried, then, consider the next transaction and go to step 5, otherwise stop the procedure.

6. Results and Discussions

This section highlights the details of the simulation carried out on IEEE 30-bus system for ATC computation under the normal operating condition and line outage condition using FPAapproach. The system data are in a per-unit system and taken from [15] and the base MVA value is taken to be 100 MVA. In the IEEE-30 bus system consists of six generators and forty-one lines are considered and shown in Fig. 2. Here, the transactions with generators connected at buses 2, 5, 8, 11 and 13 are treated as seller buses and the load buses are treated as buyer buses. Generators at buses 8, 11 and 13 are considered in area 1, while the remaining generators at buses 1, 2 and 5 are considered in area 2. The tie-line existing between the two areas and transaction is carried out between area 1 and area 2. Three inequality constraints are considered in these studies: the voltage limit, line thermal limit and reactive power generation limit.

In the OPF problem, ATC is considered as an objective. The ATC has been determined using ACPTDFs based on the line flow limit under normal and line outage conditions. The method runs for each increment of the transaction over its base value until any of the lines flows or the bus voltages hit the limiting value. A transaction is carried out between area 1 and area 2 and the voltage magnitude limit of each bus is assumed to be between 0.95 p.u and 1.05 p.u. The simulations have been carried out on a 2.40 GHz Dual-Core, Intel Pentium system in a MATLAB 2010a environment.
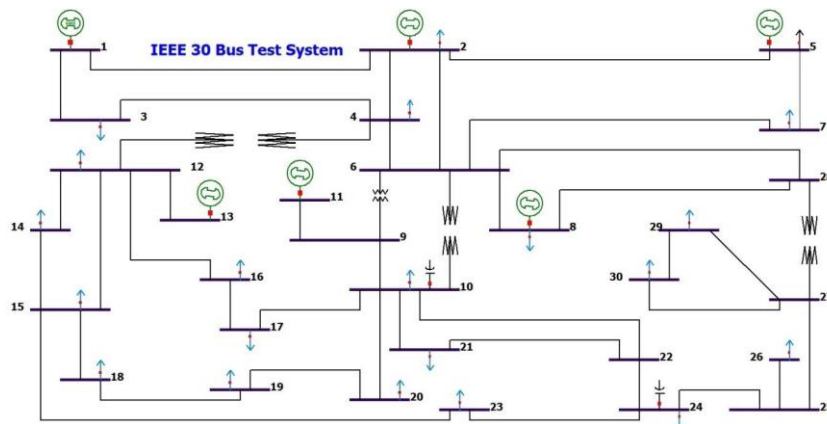

**Fig. 2. Single line diagram of the IEEE 30-bus system.**

Case 1: Normal operating conditions

In this study, ATC enhancement is obtained with the best location and sizing of TCSC devices by applying the FPA technique. Installation cost of these TCSC devices has also been calculated for each transaction with reference to ATC value. In bilateral transactions, seven transactions between a seller bus in the source area and buyer bus in sink area such as (5-30, 13-27, 5-20, 2-10, 11-27, 8-30, 8-30 and 2-23) are considered. From Table 1, by considering a bilateral transaction from bus 11 to bus 27. The best possible position of TCSC is between buses 15 and 18 and the corresponding optimal size and installation cost is -0.0541 p.u and 0.68×10^8 US $ respectively. The negative sign indicates that TCSC works in capacitive mode. The ATC value is improved from 40.89 MW to 44.78 MW after installing TCSC without violating the system constraints is shown in Table 2. Moreover, the active and reactive power loss as reduced from 10.68 MW and -3.422 MVAr to 6.923 MW, -2.942 MVAr respectively after placing TCSC is tabulated in Table 2.

The different possible combinations of multilateral transactions between seller buses in the source area and buyer buses in sink area as shown in Tables 1 and 2. From Table 1, consider a multilateral transaction from buses 5, 8, 11 to buses 27, 30. In this case, the best possible position of TCSC is between buses 15 and 23 and the optimal size and installation costs of TCSC is -0.0921 p.u and 0.78×10^8 US $. The corresponding ATC value has improved from 20.54 MW to 29.54 MW without violating system constraints is shown in Table 2. From Table 2, it can be observed that the active and reactive power loss is also reduced from 16.54 MW and -6.128 MVAr to 13.78 MW, -5.478 MVAr respectively by placing TCSC devices. The results of different bilateral and multilateral transactions are shown in Table 1 and 2 and Fig. 3. From Tables 1 and 2 and Fig. 3, it can be seen that ATC values are increased for all possible transactions and power losses are reduced after placing TCSC devices in the right location.

Case 2: Contingency operating conditions

For a contingency case, the branch line outages between buses 9-10 and 12-15 are considered. The optimal parameter of TSCS devices, ATC values and active and reactive power losses for different bilateral and multilateral transactions without and with TCSC devices are shown in Tables 3 to 6. From Tables 4 and 6, it is indicated that optimally placed TCSC devices significantly increase ATC with reduced active and reactive power losses. Moreover, the FPA technique has been highly efficient in maximizing the ATC as compared with PSO is shown in Fig. 4.
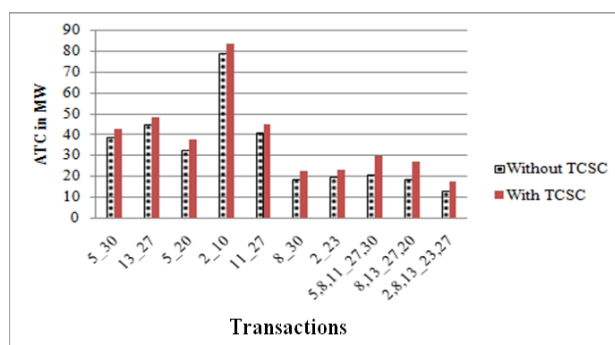
(a) ATC enhancement for IEEE-30 bus system without and with TCSC.
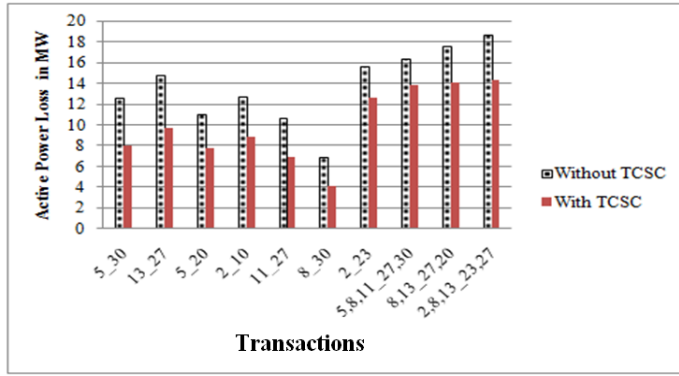
(b) Active power loss for IEEE-30 bus system without and with TCSC.
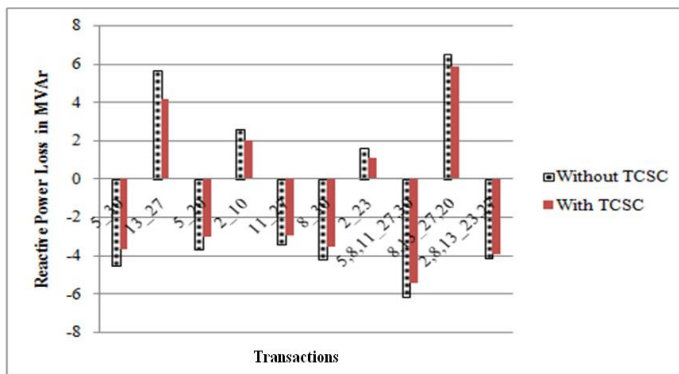
(c) Reactive power loss for IEEE-30 bus system without and with TCSC.

Fig. 3. ATC enhancement and power loss for IEEE-30 bus system without and with TCSC devices under normal operating conditions.

Fig. 4. Objective function characteristics for system and with TCSC devices using PSO and FPA technique under normal operating conditions.

Table 1. Control parameters of TCSC device with ATC enhancement for IEEE-30 bus system under normal operating conditions.

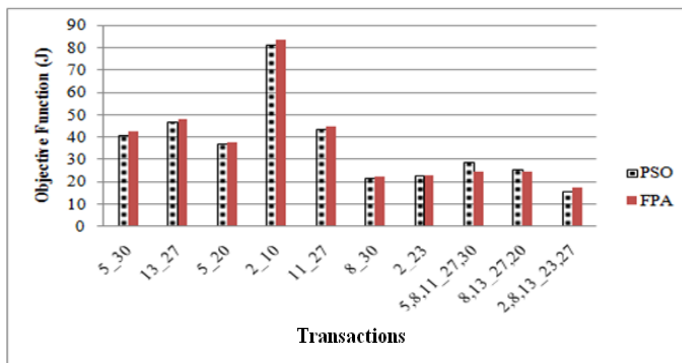| Transactions	Allocation technique	Location (line)	Size in X_{TCSC} (p.u)	Cost (US $) x$10^8$
5-30	FPA	Bus (16-12)	-0.1181	0.82
	PSO	Bus (16-12)	-0.1195	0.84
13-27	FPA	Bus (27-29)	-0.1925	1.22
	PSO	Bus (27-29)	-0.1968	1.24
5-20	FPA	Bus (15-18)	-0.1121	0.93
	PSO	Bus (15-18)	-0.1125	0.95
2-10	FPA	Bus (15-18)	-0.2162	1.17
	PSO	Bus (15-18)	-0.2171	1.21
11-27	FPA	Bus (15-18)	-0.0541	0.68
	PSO	Bus (15-18)	-0.0546	0.69
8-30	FPA	Bus (27-30)	-0.2696	1.78
	PSO	Bus (27-30)	-0.2721	1.81
2-23	FPA	Bus (15-23)	-0.1262	1.02
	PSO	Bus (15-23)	-0.1298	1.08
5, 8, 11-27, 30	FPA	Bus (15-23)	-0.0921	0.78
	PSO	Bus (15-23)	-0.0991	0.81
8, 13–27, 20	FPA	Bus (22-24)	-0.0887	0.71
	PSO	Bus (22-24)	-0.0891	0.72
2, 8, 13-23, 27	FPA	Bus (15-23)	-0.0901	0.73
	PSO	Bus (15-23)	-0.0968	0.74

Table 2. Enhancement of ATC and power loss with TCSC for IEEE-30 bus system under normal operating conditions.

Transactions	Allocation technique	ATC in MW		Active power loss in MW		Reactive power loss in MVAr	
		without TCSC	with TCSC	without TCSC	with TCSC	without TCSC	with TCSC
5-30	FPA	38.74	42.65	12.64	7.962	-4.521	-3.693
	PSO	36.65	40.81	13.12	8.131	-4.735	-3.891
13-27	FPA	44.83	47.81	14.78	9.641	5.647	4.117
	PSO	43.94	46.92	15.84	9.869	5.788	4.345
5-20	FPA	32.54	37.62	11.11	7.708	-3.689	-3.012
	PSO	31.04	36.91	12.23	8.607	-3.792	-3.108
2-10	FPA	78.71	83.46	12.79	8.811	2.612	1.978
	PSO	75.48	81.54	13.81	9.678	2.729	1.997
11-27	FPA	40.89	44.78	10.68	6.923	-3.422	-2.942
	PSO	39.91	43.94	11.71	7.678	-3.548	-2.984
8-30	FPA	18.52	22.61	6.921	4.126	-4.178	-3.587
	PSO	17.98	21.96	7.931	5.137	-4.281	-3.633
2-23	FPA	19.54	23.01	15.62	12.62	1.612	1.078
	PSO	18.92	22.85	16.68	13.21	1.727	1.091
5, 8, 11-27, 30	FPA	20.54	29.54	16.54	13.78	-6.128	-5.478
	PSO	19.81	28.69	17.49	14.36	-6.341	-5.612
8, 13–27, 20	FPA	18.63	26.72	17.61	14.07	6.534	5.818
	PSO	17.87	25.69	18.66	15.58	6.667	5.945
2, 8, 13-23, 27	FPA	12.84	17.54	18.67	14.32	-4.137	-3.978
	PSO	11.98	16.04	19.74	16.64	-4.256	-3.987

**Table 3. Control parameters of TCSC device with ATC enhancement
for IEEE-30 bus system under contingency operating conditions
(with line outage of 9-10).**

Transactions	Control parameters of TCSC devices with enhancement of ATC			
	Allocation technique	Location (line)	Size in X_{TCSC} (p.u)	Cost (US $) x10^8
5-30	FPA	Bus (16-12)	-0.1257	1.01
	PSO	Bus (16-12)	-0.1264	1.02
13-27	FPA	Bus (27-29)	-0.2144	1.14
	PSO	Bus (27-29)	-0.2153	1.15
5-20	FPA	Bus (15-18)	-0.1281	1.05
	PSO	Bus (15-18)	-0.1292	1.06
2-10	FPA	Bus (16-17)	-0.2372	1.28
	PSO	Bus (16-17)	-0.2458	1.31
11-27	FPA	Bus (6-28)	-0.0723	0.71
	PSO	Bus (6-28)	-0.0778	0.74
8-30	FPA	Bus (27-30)	-0.2725	1.79
	PSO	Bus (27-30)	-0.2884	1.81
2-23	FPA	Bus (15-23)	-0.1262	1.08
	PSO	Bus (15-23)	-0.1333	1.11
5, 8, 11- 27, 30	FPA	Bus (22-21)	-0.1062	0.81
	PSO	Bus (15-18)	-0.1038	0.84
8, 13–27, 20	FPA	Bus (15-18)	-0.1032	0.77
	PSO	Bus (15-18)	-0.1064	0.82
2, 8, 13-23, 27	FPA	Bus (15-23)	-0.1071	0.85
	PSO	Bus (15-23)	-0.1073	0.87

**Table 4. Enhancement of ATC and power loss with TCSC
for IEEE-30 bus system under contingency operating conditions
(with line outage of 9-10).**

Transactions		ATC in MW		Active power loss in MW		Reactive power loss in MVAr	
	Allocation technique	without TCSC	with TCSC	without TCSC	with TCSC	without TCSC	with TCSC
5-30	FPA	17.63	24.54	13.78	8.869	-6.521	-4.875
	PSO	16.62	23.61	14.84	9.458	-7.648	-5.978
13-27	FPA	22.12	26.37	15.82	10.82	-7.647	-5.305
	PSO	21.24	25.45	16.97	11.64	-8.789	-6.218
5-20	FPA	14.78	19.17	12.23	8.804	-5.689	-4.147
	PSO	13.81	18.33	13.36	9.045	-6.789	-5.328
2-10	FPA	15.15	18.62	13.91	9.904	-4.612	-2.997
	PSO	14.27	17.71	14.89	10.12	-5.758	-3.478
11-27	FPA	26.38	29.64	12.72	7.947	-5.422	-3.987
	PSO	25.38	28.72	13.84	8.881	-6.381	-4.548
8-30	FPA	17.51	20.17	8.945	6.247	-6.178	-4.657
	PSO	16.56	19.34	9.962	7.203	-7.237	-5.258
2-23	FPA	15.67	19.68	16.71	13.79	-2.612	-2.178
	PSO	14.56	18.79	17.87	14.21	-3.458	-3.078
5, 8, 11-27, 30	FPA	18.45	23.14	18.55	15.94	-8.128	-6.078
	PSO	16.45	22.78	19.71	17.12	-9.333	-7.117
8, 13–27, 20	FPA	17.58	22.37	18.82	16.47	-8.534	-6.423
	PSO	16.61	21.55	19.57	17.84	-9.345	-7.158
2, 8, 13-23, 27	FPA	11.14	15.66	19.73	16.64	-6.137	-5.071
	PSO	10.96	14.71	20.37	17.91	-7.012	-6.123

**Table 5. Control parameters of TCSC device with ATC enhancement for
IEEE-30 bus system under contingency operating conditions
(with line outage of 12-15).**

Transactions	Control parameters of TCSC devices with enhancement of ATC			
	Allocation technique	Location (line)	Size in X_{TCSC} (pp.)	Cost (US $) $x10^8$
5-30	FPA	Bus (12-14)	-0.1357	1.02
	PSO	Bus (12-14)	-0.1395	1.05
13-27	FPA	Bus (27-30)	-0.2645	1.18
	PSO	Bus (27-30)	-0.2693	1.19
5-20	FPA	Bus (18-19)	-0.1245	1.01
	PSO	Bus (18-19)	-0.1257	1.02
2-10	FPA	Bus (4-6)	-0.1152	1.04
	PSO	Bus (4-6)	-0.1161	1.04
11-27	FPA	Bus (6-7)	-0.0834	0.81
	PSO	Bus (6-7)	-0.0891	0.84
8-30	FPA	Bus (27-29)	-0.2875	1.82
	PSO	Bus (27-29)	-0.2978	1.82
2-23	FPA	Bus (15-23)	-0.1378	1.12
	PSO	Bus (15-23)	-0.1462	1.13
5, 8, 11-27, 30	FPA	Bus (22-21)	-0.1123	0.97
	PSO	Bus (22-21)	-0.1187	0.98
8, 13–27, 20	FPA	Bus (15-18)	-0.1069	0.89
	PSO	Bus (15-18)	-0.1097	0.91
2, 8, 13-23, 27	FPA	Bus (15-23)	-0.1105	0.98
	PSO	Bus (15-23)	-0.1214	1.09

**Table 6. Enhancement of ATC and power loss with TCSC
for IEEE-30 bus system under contingency operating conditions
(with line outage of 12-15).**

Transactions		ATC in MW		Active power loss in MW		Reactive power loss in Mar	
	Allocation technique	without TCSC	with TCSC	without TCSC	with TCSC	without TCSC	with TCSC
5-30	FPA	28.68	31.78	15.78	10.57	-5.458	-4.367
	PSO	23.67	28.97	16.64	12.78	-6.123	-5.782
13-27	FPA	24.83	29.86	13.12	10.07	6.345	5.158
	PSO	23.94	27.52	13.98	11.12	6.878	5.824
5-20	FPA	28.55	32.64	10.57	8.708	-4.745	-3.075
	PSO	27.57	31.78	11.01	9.107	-4.792	-3.208
2-10	FPA	38.67	40.78	13.79	11.57	3.678	2.611
	PSO	35.32	37.45	14.81	12.78	3.894	2.872
11-27	FPA	26.64	28.51	12.01	9.243	-6.345	-5.678
	PSO	25.18	27.72	12.97	9.695	-6.887	-5.945
8-30	FPA	20.97	21.58	9.012	6.578	-6.458	-4.788
	PSO	19.71	20.02	9.348	7.112	-7.345	-5.978
2-23	FPA	18.74	19.12	11.76	10.17	-3.978	-3.062
	PSO	16.63	17.58	12.08	10.87	-4.857	-4.245
5, 8, 11- 27, 30	FPA	19.62	21.67	15.61	14.12	-9.458	-8.756
	PSO	18.31	20.24	16.84	15.27	-9.978	-8.997
8, 13–27, 20	FPA	18.58	20.51	16.13	15.32	-10.24	-9.785
	PSO	17.97	19.59	17.66	16.74	-10.78	-9.978
2, 8, 13-23, 27	FPA	12.14	13.75	16.84	15.52	-8.678	-7.125
	PSO	11.99	12.81	17.47	16.76	-8.971	-7.344

7. Conclusions

ATC Enhancement is an important issue in a deregulated power system. Furthermore, Optimum utilization of the transmission lines available capacity indicates the necessity of implementing series FACTS devices in the power grid. In this paper, a methodology to evaluate ATC using sensitivity factors approach has been presented. The ATC value is further enhanced using Flower Pollination Algorithm based on the optimal placement and sizing of the TCSC device. From the results obtained, it is established that TCSC significantly enhances ATC and reduces total losses under the normal operating condition and line outage condition. Thus, it can be inferred that TCSC devices are efficient in Congestion Management and existing installations can be used to enhance ATC wherever congestion occurs. Moreover, FPA is able to find out the optimal location TCSC device gives better results compared to the results obtained using the PSO technique.

Nomenclatures

R	Resistance in Ω
X_C	Capacitive reactance in Ω
X_L	Inductive reactance in Ω
ΔP	Changing in real power in p.u
ΔQ	Changing in reactive power in p.u
Δt_k	change in real power transactions between the above seller and buyer in p.u
ΔV	Changing in bus voltage in p.u

Abbreviations

AI	Artificial Intelligence
ATC	Available Transfer Capability
CBM	Capacity Benefit Margin
DISCO	Distribution Companies
ETC	Existing Transmission Commitment
FACTS	Flexible Alternative Current Transmission System
FPA	Flower Pollination Algorithm
GA	Genetic Algorithm
GENCO	Generation Companies
IC	Installation Cost
ISO	Independent System Operator
L	Inductance
MVAr	Mega Volt Ampere Reactive
MW	Mega Watt
NRLF	Newton Raphson Load Flow
OPF	Optimal Power Flow
PSO	Particle Swarm Optimization
PTDFs	Power Transfer Distribution Factors
TRM	Transmission Reliability Margin
TTC	Total Transfer Capability

References

1. Sambasivarao, N.; Amarnath, J.; and Purnachandrarao, V. (2013). Enhancement of available transfer capability in deregulated power system using series FACTS device. *International Journal of Engineering Research & Technologies*, 2(11), 192-199.

2. Rao, M.V.; Sivanagaraju, S.; and Suresh, C.V. (2016). Available transfer capability evaluation and enhancement using various FACTS controllers: Special focus on system security. *Ain Shams Engineering Journal*, 7(1), 191-207.

3. Ajjarapu, V.; and Christy, C. (1992). The continuation power flow: A tool for steady state voltage stability analysis. *IEEE transactions on Power Systems*, 7(1), 416-423.

4. Ejebe, G.C.; Waight, J.G.; Sanots-Nieto, M.; and Tinney, W.F. (2000). Fast calculation of linear available transfer capability. *IEEE Transactions on Power Systems*, 15(3), 1112-1116.

5. Kumar, A.; Srivastava, S.C.; and Singh, S.N. (2004). Available transfer capability (ATC) determination in a competitive electricity market using AC distribution factors. *Electric Power Components and Systems*, 32(9), 927-939.

6. Wu, Y.K. (2007). A novel algorithm for ATC calculations and applications in deregulated electricity markets. *International Journal of Electrical Power & Energy Systems*, 29(10), 810-821.

7. Shweta; Nair, V.K.; Prakash, V.A.; Kuruseelan, S.; and Vaithilingam, C. (2017). ATC evaluation in a deregulated power system. *Energy Procedia*, 117, 216-223.

8. Xiao, Y.; Song, Y.H.; Liu, C.-C.; and Sun, Y.Z. (2003). Available transfer capability enhancement using FACTS devices. *IEEE Transactions on Power Systems*, 18(1), 305-312.

9. Albatsh, F.M.; Mekhilef, S.; Ahmad, S.; Mokhlis, H.; and Hassan, M.A. (2015). Enhancing power transfer capability through flexible AC transmission system devices: A review. *Frontiers of Information Technology & Electronic Engineering*, 16(8), 658-678.

10. Babu, T.G.; and Srinivas, G.N. (2017). Enhancement of ATC with FACTS device using firefly algorithm. *International Journal of Applied Engineering Research*, 12(20), 10269-10275.

11. Nireekshana, T.; Rao, G.K.; and Raju, S.S.N. (2012). Enhancement of ATC with FACTS devices using real-code genetic algorithm. *International Journal of Electrical Power & Energy Systems*, 43(1), 1276-1284.

12. Chansareewittaya, S.; and Jirapong, P. (2015). Power transfer capability enhancement with multitype FACTS controllers using hybrid particle swarm optimization. *Electrical Engineering*, 97(2), 119-127.

13. Esmaeili, A.; and Esmaeili, S. (2013). A new multi objective optimal allocation of multitype FACTS devices for total transfer capability enhancement and improving line congestion using the harmony search algorithm. *Turkish Journal of Electrical Engineering & Computer Sciences*, 21(4), 957-979.

14. Reddy, S.S.; Kumari, M.S.; and Sydulu, M. (2010). Congestion management in deregulated power system by optimal choice and allocation of FACTS controllers using multi-objective genetic algorithm. *Proceedings of the* IEEE

Power and Energy Society (PES) *Transmission, Distribution and Exposition Conference*. New Orleans, Louisiana, United States of America, 1-7.

15. Manikandan, B.V.; Raja, S.C.; and Venkatesh, P. (2011). Available transfer capability enhancement with FACTS devices in the deregulated electricity market. *Journal of Electrical Engineering & Technology*, 6(1), 14-24.

16. Yang, X.-S. (2012). Flower pollination algorithm for global optimization. *Proceedings of the 11th International Conference on Unconventional Computing and Natural Computation*. Orlean, France, 240-249.

17. Yang, X.-S.; Karamanoglu, M.; and He, X. (2014). Flower pollination algorithm: A novel approach for multi objective optimization. *Engineering Optimization*, 46(9), 1222-1237.